“Babeș-Bolyai” University Cluj-Napoca

Faculty of Geography

Doctoral School of Geography

URBAN HEAT ISLAND IN CLUJ-NAPOCA CITY. EVALUATION AND SUSTAINABLE MITIGATION TECHNIQUES.

-abstract-

Scientific adviser:

Professor Dănuț Petrea, PhD

PhD Candidate:

Ioana Herbel

Cluj-Napoca
2020

TABLE OF CONTENTS:

Keywords: *Cluj-Napoca, urban heat island (UHI), Landsat, land surface temperature, UHI mittigation*

1. INTRODUCTION

The expansion without precedent of city boundaries determines the modification of the climatic conditions inside the cities, with a direct impact on the environment and the population. The urban development implies fundamental changes on the natural setting, generating significant differences between the urban environment and the nearby areas regarding the meteorological parameters, the air quality and the energy balance.

Over the last decades, cities worldwide have experienced an accelerated development, urbanization being on the most important dimensions of global change. Nowadays, 54% of the world population lives in urban areas, being responsible for 76% of the energy consumption and emissions of greenhouse gasses (Grubler *et al.* 2012). Moreover, by 2050 the urban population is expected to grow by 66% (United Nations and Department of Economic and Social Affairs 2014). This also entails the expansion of the urban tissue and a massive growth for built surface demand in the following decades (Seto, Güneralp, and Hutyra 2012; Song *et al.* 2016).

According to the European Environment Agency (EEA), in Europe alone, 73% of the population lives in cities (EEA, 2010) and it is expected to grow to 82% by 2020 (Akbari *et al.* 2016). A report of the World Bank nominates the secondary cities (like Cluj-Napoca) as one of the main engines of growth in the European Union (Cristea *et al.* 2017). The optimistic scenario of this report forecasts a doubling of the population in Cluj-Napoca, the study area of the present research. Here, as well as in other Eastern-European cities, another important topic related to our research problem is the forced industrialization from the communist era, which lead to a complex process of urban change in post-socialist cities, influencing in the same time the urban climate. The urban landscape was radically transformed with the emergence of over-sized production units and the "dormitory neighborhoods" meant to accommodate their personnel. The replacement of natural surfaces with the built, impervious ones (with distinct caloric properties and smaller cooling rates), is known as one of the main factors that cause the urban heat island effect.

Study area

Cluj County is located in the northwestern part of Romania, at the intersection of three main natural units: the Apuseni Mountains, the Someșan Plateau, and the Transilvanian Plain. Concerning the relief, it is characterized mainly by hills that cover more than two thirds from its surface.

Cluj-Napoca is the county seat and a rank I municipality, according to the Law 351/2001. Located in the central part of Cluj County (46° 46′ N and 23° 36′ E) at an average altitude of 360 m, the city covers a surface of 179.5 square kilometers. Placed along Someșul Mic, on one side and another of the meadow, the terrace complex is distributed. It covers the largest part of the depressionary corridor ("General Memoire for the General Urban Plan of Cluj-Napoca Municipality" 2012).

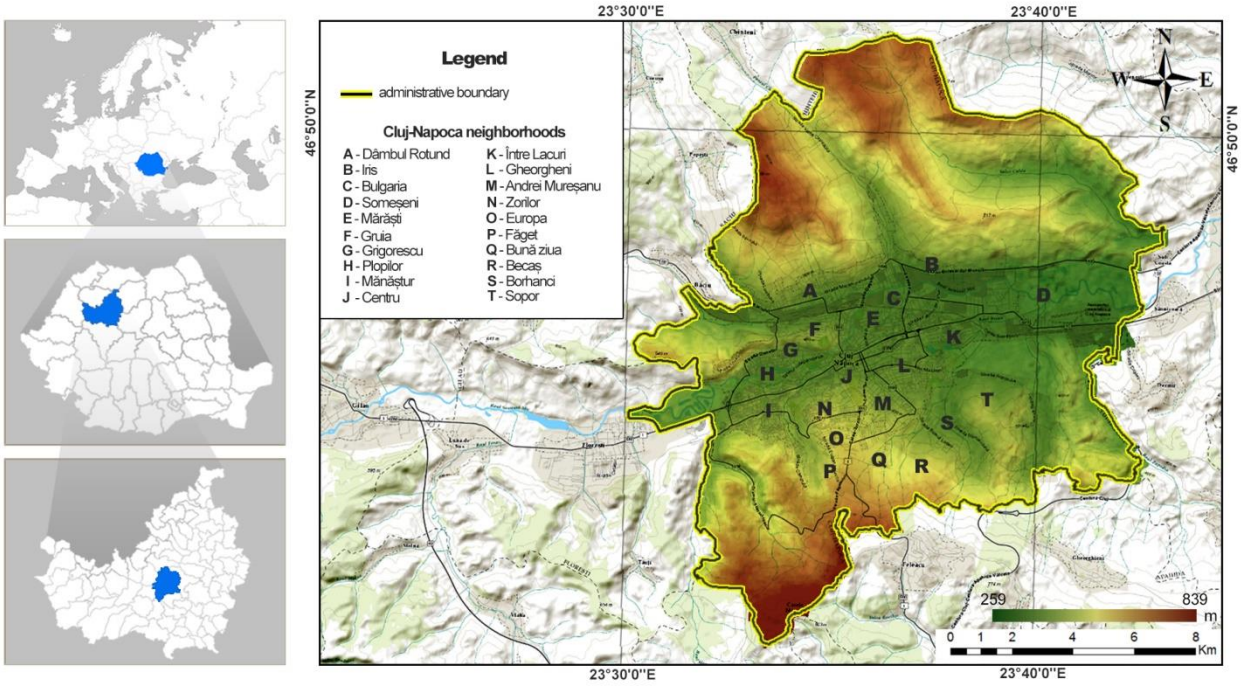

Figure 1.1 The presentation of the study area and its districts (source: Herbel *et al*. 2017)

In the Southwestern side, it covers the space of the superior terrace of the Northern slope of Feleac, being surrounded in three parts by hills with heights between 500 and 839 m (Fig. 1). On the Southern side, the city is bordered by the Feleac hill, with a maximum altitude of 825 m in Măgura Sălicei peak. On the Eastern side, the Someșan Plain can be observed, while in the North we can find the hills of Cluj with maximum altitudes in Dealul Lombului (648 m) and Dealul Melcului peaks (617 m). Other hills nearby are Hoia (506 m) and Gârbău (570 m), while inside the city Calvaria and Cetățuia hills can be found ("General Memoire for the General Urban Plan of Cluj-Napoca Municipality" 2012).

The hydrography plays an extremely important role in regulating the air temperature. From this point of view, Cluj County is characterized by a rich network of rivers, lakes and underground resources. Cluj-Napoca extends on the valleys of Someșul Mic and Nădaș rivers, with some

extensions on the secondary valleys of ale Popești, Chintău and Borhanci. The most important hydrographic element is Someșul Mic river, that crosses the city from west to east over a length of 16 km. It has many affluents like the brooks Gârbău, Becaș, Murători, Zăpodie, Calvaria, Plopilor, Țigani I and Țigani II ("General Memoire for the General Urban Plan of Cluj-Napoca Municipality" 2012).

The Aeolian regime, because of the relatively low frequency and wind speed, does not present special problems. The depressionary aspect of the relief largely influences the temperature regime by favoring the stagnation of the cool air near the bottom, an aspect that favors frequently the formation of temperature inversions (Belozerov 1972).

On this background of the general climate, a diversity of topo- and microclimate is differentiated, determined by the specificity of the active surface. The features of the various surfaces, the orientation, slope, air circulation and exposition to sun rays determine the apparition in Cluj-Napoca of four topoclimatic sectors: Northern slope, Southern slope, meadow and anthropic (Irimuș *et al.* 2010).

From a demographic point of view, Cluj-Napoca city has experienced accelerated growth in the last century, the number of inhabitants being five times higher than in 1912. The city population has a spectacular growth in the communist era. This situation can be attributed to forced industrialization, but also to the pronatalist policies sustained by the communist regime that have as starting point the Decree 770/1966 (the abortion is forbidden). A more numerous population demands the fast construction of new houses. This is the context of the apparition of dormitory neighborhoods. They determine the urban geometry, one of the main factors influencing the UHI. In the past 20 years, the population has stabilized around 300.000 inhabitants, with a descending trend in the last years. According to the last census from 2011, the population of the municipality consists of 309.136 inhabitants. As one of the most important academic and cultural centers in the country, the city also attracts a floating population of students, approximately 70.000 every year ("General Memoire for the General Urban Plan of Cluj-Napoca Municipality" 2012).

2. URBAN HEAT ISLAND. THEORETICAL ASPECTS.

UHI: Definition, classification, variations.

The accelerated urbanization from the last decades, materialized through the rapid expansion of city boundaries, also determined the warming of the urban climate. This phenomenon involves the concentration of high air (but surface as well) temperatures in the shape of an island (Sailor 1995). The peri-urban and rural areas around the city, stay cooler. If the structure is a multicellular one, we can even refer to an archipelago of urban heat (Unger 2004).

The UHI can manifest at the level of surfaces (natural or built) and at air level. In the first case, we can refer to the surface urban heat island (SUHI), while in the second to the atmospheric urban heat island (AUHI). SUHIs occur day and night, are more intense in the summer days and can be identified based on satellite image data in thermal infrared domain. AUHIs are more intense during the night, in the summer and winter, and can be evaluated through direct measurements, in fixed points and/or by mobile transverses performed using different transportation means. During the day, the expansion and intensity of AUHI is variable and can be modified because of the buildings that shade areas.

UHIs are characterized by periodic and aperiodic variations. The diurnal variations are very pronounced. During the day, the temperature differences between the urban areas and the nearby rural ones, even during sunny, calm days are very small. In some situations, the measurements performed at airports near cities can have higher thermic values than some areas from inside the city (Landsberg 1981).

While SUHIs are present day and night, but more intense in the afternoon, AUHIs have sometimes a smaller intensity by liberating the heat stored in the urban structures (Hove 2011). The moment of this peak depends on the properties of the urban and rural surfaces, on the season and on the weather conditions from the data collection time (Hashem *et al.* 2016).

Regarding the temperature differences by seasons, these are more intense during the summer and winter. The highest differences have been observed during long summer nights, in anticyclonic weather conditions, when the sky is clear and the atmospheric calm predominates (Landsberg 1981).

Causes of the heat island development in urban areas

The UHI genesis is related to controllable and uncontrollable factors. When it comes to controllable factors, we first mention the characteristics of the urban surfaces and their structure (city geometry). Correlated with the reduced green space areas, these features largely influence the heat island intensity. Human activity inside the cities generates the so-called anthropogenic heat, a source often nominated in the literature as main cause of the UHI effect. Atmospheric pollution contributes also to the heat island, because the air particles absorb and emit radiation inside the city (Gartland 2008).

The urban geometry

The fact that the most significant changes of the radiation quantity inside the city are generated by the properties of the urban surface, characterized by structural discontinuity (buildings, streets, green spaces) and by varied shapes, cannot be questioned (Fărcaș 1999).

The urban structures store a large quantity of heat during the day, that is slowly released during the night as infrared radiation. The buildings and pavements (especially the ones made from dark-colored materials) form true canyons that maintain the sun energy in the volume delimited by the urban structure elements.

The city geometry exerts a major influence on the urban atmosphere and has a decisive role in heat island genesis. The solar radiation (ultraviolet, visible and near infrared) is subjected during the day (in the space delimited by the urban structures) to successive reflections, that will finally lead to the absorption of the radiation by the building walls (Kleerekoper *et al.* 2012). Afterwards, it will be released through thermal transfer processes, like convection, conduction and re-radiation.

Characteristics of the urban surfaces

The heating effect inside the city is due to a mix of factors, more than individual causes. One of the most important aspects related to the UHI genesis is the replacement of natural surfaces with built ones, with different caloric properties and cooling rates. The natural surfaces are mostly made of vegetation and soils that absorb the moist, with a regulating effect on the air temperature. These land cover types use a large part of the radiation for evapotranspiration, releasing water vapors that cool the surfaces that they come in contact with. On the other hand, artificial surfaces are impervious and characterized by properties that favor the apparition of heat islands, like low reflectivity and higher thermal diffusivity.

One of the main influencing factor is the *permeability degree of surfaces*. The materials from the urban environment are impervious, leading to the modification of the urban energy balance, but also to the overload of the sewer system during periods with abundant precipitations. These materials cannot dissipate heat by evaporation and warm the air above, especially during the night when the urban heat is released slowly by urban structures.

The main factor influencing the amount of radiation stored by the urban surfaces is their reflectivity. The albedo is a measure of surface reflectivity. It can be defined as the ratio between the reflected radiation and the incident radiation on a certain surface. Some researchers (Oke 1982) consider that UHI has as main cause the fact that the cities tend to have a lower albedo than the nearby rural areas.

Anthropogenic heat

The UHI is strongly influenced by the anthropogenic heat. This type of heat is generated by the human activity inside the cities that modify the balance of urban energy. The anthropogenic heat has many sources, but the main producers are transportation and heating installations, air conditioning systems and industrial processes.

The magnitude of the anthropogenic heat flux depends first on the population density, but also on the *per capita* energy consumption (Oke 1988).

Uncontrollable factors

The UHI intensity depends of uncontrollable factors of meteorological nature like the low wind speed and the cloud cover *(cloudiness),* because these parameters regulate the amount of radiation that reaches the Earth's surface and minimize the release of radiation through heat transfer processes, like convection. Low wind speeds or situations with atmospheric calm remove heat slower. Clear sky and calm winds represent proper conditions for the apparition of UHI, while a high cloud cover degree and strong winds suppress it.

UHI is also influenced by the geographic position. The presence of large water bodies near the cities influence the urban temperature and generates winds. Such air currents determine the convection of heat outside the urban areas. The mountains nearby can prevent the winds to reach inside the cities or even create crossing patterns.

3. EVALUATION METHODS OF UHI. A LITERATURE REVIEW.

In the literature, the evaluation of the effects of development on the urban climate is traditionally obtained by 5 different methods, with direct or indirect data gathering: fixed station/point, mobile transverses, energy balances, remote sensing and vertical sensing (Gartland 2008a). The first three are used for the evaluation of AUHI and the other two are specific to SUHI.

3.1 AUHI evaluation in the literature.

The exploration of the spatial and temporal characteristics of AUHI can be performed by using any of the first three methods presented above. Therefore, AUHI can be detected by measurements in fixed points, mobile transverses and energetic balances.

3.1.1 Measurements in fixed points

3.1.1.1 Urban-rural station pairs

The simplest method to evaluate the impact of development on the urban climate consists in comparing the temperature values recorded in two fixed points, one from the urban environment and the other from the nearby rural area. The use of such data requires a close attention because the observation points from inside and outside the cities must be representative for the studied phenomena.

3.1.1.2 Networks of points

A more complex analysis of AUHI is based on data collected by more meteorological stations in the urban environment. These is preferable to the first method because AUHI can easily be mistaken with thermal advection or thermal inversions, especially if its intensity is calculated based on the temperature difference between an urban-rural pair of points.

3.1.2 Mobile transverses

Temperature measurements on pre-established routes with stops in representative points are an efficient way to explore the spatial and temporal characteristics of AUHI. This can be easily achieved with only one set of instruments. In order to move from one point of interest to another, in urban climate studies, researchers use cars, public transportation or even bikes.

3.1.3 Energy balances

Energy balances represent a more sophisticated method for measuring atmospheric urban heat islands. However, due to logistics and methodological problems, there are very few studies in the literature that use this method in the densely built urban areas.

3.2 SUHI evaluation

The study of SUHI has spread along with the technology development in the field of remote sensing which opened new perspectives for urban climatology. The capacity of different sensors to offer data at a high spatial resolution in thermal infrared became very attractive and valuable for this domain.

In order to detect SUHI by processing thermal infrared satellite image data, many studies use the land surface temperature (LST), a defining parameter for the urban climate.

To examine the spatial patterns of SUHI, images captured by many different sensors, either satellite or airborne, are currently available. The airborne sensors are fixed onboard of planes or helicopters.

3.2.1 Radiometric data acquisition using airborne sensors

Mapping the surface temperature with planes or helicopters equipped with thermal sensors has the advantage of acquiring data at a high spatial resolution compared to satellite data because of the lower altitude. The vast majority of the studies that evaluate UHI don’t use thermal radiometry with airborne sensors independently, but in association with other specific methods.

3.2.2 SUHI evaluation based on satellite image

Examining the spatial patterns of SUHI is usually performed in the literature based on images provided by satellite sensors of low (MODIS, AVHRR) and average (Landsat, ASTER) spatial resolution. LST can be derived from ASTER, AVHRR and MODIS spatial data with all of the specific methods due to their multiple thermal bands.

3.2.2.1 Computing LST from MODIS imagery

MODIS is an instrument fixed onboard Terra and Aqua satellites that record data in 36 wavelength groups (three from the spectral region) at a spatial resolution between 250 and 1000 meters. The orbit of Terra is synchronized so that the satellite transverses the Earth from north to south over the Equator in the morning, while Aqua crosses over this region from south to north in the afternoon. The two satellites visualize the entire Earth surface once every 1-2 days.

3.2.2.2 Computing LST from AVHRR imagery

The AVHRR radiometer is a radiation detector that can be used for determining the cloudiness, as well as the Earth's surface temperature, water bodies or even cloud temperature. The instrument contains detectors that collect data in six wavelength groups. From these groups, three are located in the thermal region of the infrared domain.

3.2.2.3 Computing LST from ASTER imagery

ASTER radiometer is a multispectral sensor placed onboard Terra satellite, with 14 bands (five of them are in the thermal region) that provide image data with a spatial resolution between 15 and 90 meters. It is also one of the main instruments used in the literature for investigating the SUHI phenomenon. Therefore, the surface temperature can be easily obtained from these products with a hybrid algorithm developed by the team project that uses spectral contrast, separating the temperature and emissivity (TES).

3.2.2.4 Computing LST from Landsat imagery

Because of the technical characteristics and the high accessibility of satellite scenes, the vast majority of studies use Landsat imagery in the evaluation of SUHI. The main topics addressed in the literature refer to the temporal variation of SUHI, to the examination of the spatial structure of the island in relation to the urban surface characteristics (5-8 land cover/ land use classes), as well as to the relation of the surface temperature with different indices (especially the vegetation ones).

3.2.2.5 Multi-sensor approach

At the present moment there does not exist any satellite sensor that provides qualitative data from all point of view. Medium resolution satellite sensors (like ASTER and Landsat) have a low revisiting time, approximately 15 days. On the other hand, the sensors with high revisiting time (like AVHRR and MODIS) provide low resolution imagery. Therefore, some researchers have adopted a multi-sensor approach that combines thermal infrared satellite scenes from different sensors.

3.3 Evaluation of UHI using mixed methods

The research of the spatial and temporal variations of SUHI or AUHI can be performed by mixed methods as well. In the literature, using this approach has as a main objective the identification of the correlation degree between AUHI and SUHI, but also a more precise characterization of the phenomenon. Mixed methods can be applied either for AUHI identification,

either for the simultaneous evaluation of both ways of manifestation of UHI. They usually imply stationary measurements, mobile transverses and radiometric measurements. In the literature, different associations of these methods have been identified.

3.3.1 The SUHI-AUHI relation

One of the main research topics from thermal infrared remote sensing is focused on the AUHI-SUHI relation and entails empirical or urban atmospheric models with radiometric measurements, from satellite or *in situ*, collected simultaneously. Even if the vast majority of studies identify a positive relation between the two parameters, the AUHI-SUHI link remains an empirical one. Until this point, a simple general relation has not been identified.

3.3.2 The integrated approach of UHI

Using mixed methods for obtaining an overview on UHI is another practice found often in the literature.

3.4 UHI evaluation in Romania

A limited number of studies focused on UHI have been initiated until now in Romania. The vast majority of them were performed in Bucharest and the capital's metropolitan area. They are focused mainly on SUHI evaluation, but some of the studies examine AUHI as well.

In Cluj-Napoca city, the research of UHI were accomplished during the present doctoral studies. In 2014, Imbroane *et al.* (2014) have analyzed SUHI with Landsat satellite image data and GIS techniques, observing important differences between built central areas and the peripheral ones. The research performed by Herbel *et. al* (2016) highlight for the first time the presence of AUHI in the municipality. Later, the impact of heat waves on SUHI and local economy during three heat events from the summer of 2015 was examined by Herbel *et al.* (2017). The results shall be presented in more detail in the "Results" chapter.

4. DATA AND METHODS. THE RESEARCH DESIGN USED FOR THE EVALUATION OF UHI

The present chapter details the research design proposed in order to achieve the scientific objectives of the paper: AUHI and SUHI evaluation in Cluj-Napoca city, as well as the impact of heat waves on the surface temperature in the study area.

4.1Data and instruments used for the research

4.1.1 Data types used in the research and their source

4.1.1.1. The values of the meteorological parameters

In order to evaluate the intensity and the spatial extent of AUHI, direct measurements of the air temperature at 1.5 m from the terrain level have been performed, in seven fixed points (Figure 4.1) and on three profiles (Figure 4.2), during seven measurement campaigns.

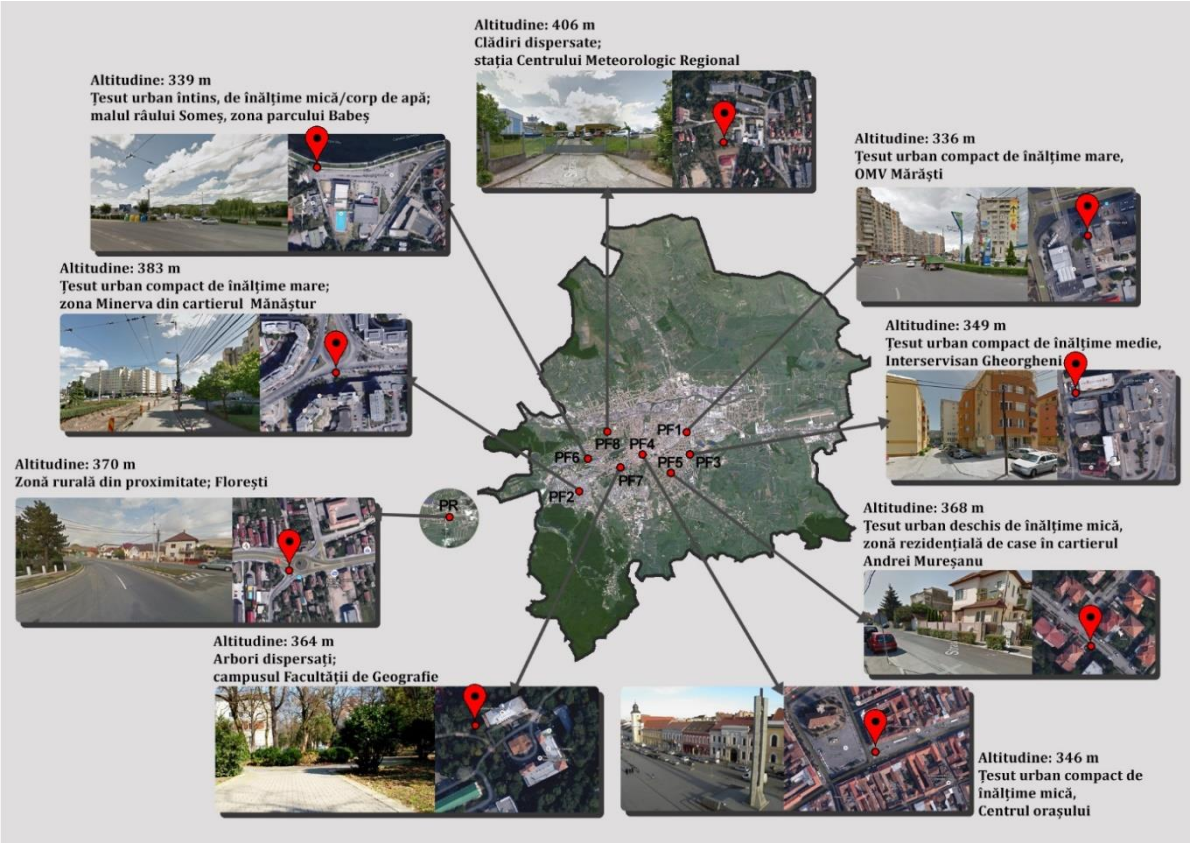

Figure 4.1 The fixed points where measurements were performed and their local climate zones

The data was collected during May 2015 – February 2016, in 7 measurement campaigns. The time of the measurements has been chosen so that the data is representative for every one of the four seasons, in synoptic weather conditions that favor the best identification of AUHI: high-pressure system (anticyclonic) and clear sky. Two measurement campaigns were performed for every season except the winter when, because of the manual collection of the temperature values along in cold weather, only one set of data has been succesfully obtained. The temperature values were recorded during weekdays but also in the weekend, in high pressure conditions, with clear sky and low wind

speeds, known to favor the manifestation of UHI. The vast majority of the campaigns took place during the night (when the atmospheric stability is the highest) between 11:00 PM and 03:00 AM (Romanian time), but in May 13-14, 2015, the temperature values were collected for 24 hours.

Besides the observations in the fixed points, during the seven campaigns, measurements were made as well on three different routes, from East to West (AA' profile, from Traian Vuia street in the vicinity of the airport to the roundabout in Florești village), fromNnorth to South (CC' profile, from Oașului street to Feleac) and from North-west to South-east (BB' profiel, from Baciu village to Colonia Borhanci).

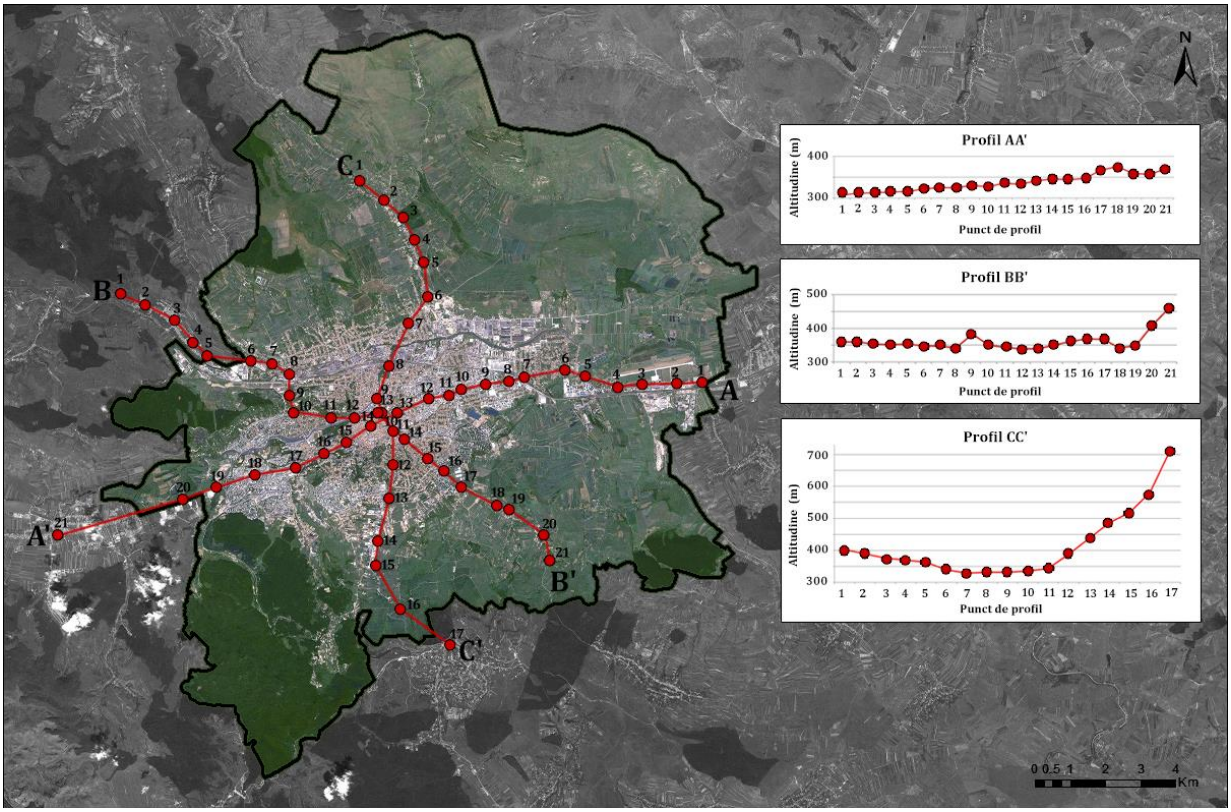

Figure 4.2 Mobile transverse routes

The three routes were covered by car, with many stops along the way, depending the changes observed in the urban tissues (between 17 and 22 points for each profile, with a variable distance); the observations on each of the profiles lasted about three hours. The most representative for AUHI detection is AA' because of the low altitude difference (62 meters), while the least representative one is CC' (380 meters difference) (Herbel *et al.* 2016). In the absence of atmospheric sounding to provide information regarding the value of the thermal gradient, this high variation of the altitude can lead to

errors in AUHI intensity evaluation. Even so, this third route was kept because it offers relevant information concerning some types of urban tissue.

The surface conditions (temperature, pressure and relative humidity of the air) needed for the correction of the spectral radiance measured by the sensor were obtained from the Cluj-Napoca Meteorological Station, from the electronic archive of the website Reliable Prognosis (http://rp5.ru). This station (WMO code 15120) belongs to the national meteorological network of the National Meteorological Administration in Romania.

The intervals with heat waves were identified based on the daily maximum temperatures recorded at the same station and provided by the project *Extreme meteorological phenomena associated to air and atmospheric precipitation in Romania* (FMETPRO) (Croitoru *et al.* 2018).

4.1.1.2 Synoptic maps

When choosing the intervals for the direct measurements and UHI analysis in heat wave conditions, the synoptic (diagnostic) analysis was performed based on sea level pressure and geopotential at 500 hPa, extracted from the electronic archive of the Meteorological Center in Karlsruhe (http://www.wetterzentrale.de), as well as on soil pressure maps provided by Met Office (http://www.metoffice.gov.uk).

Since the direct measurements took place during the night and the satellite image data was captured at noon, maps valid for 00:00 and 12:00 UTC were employed.

4.1.1.3 Satellite image data

The land surface temperature (LST), as a SUHI indicator, was computed based on image data acquired in Landsat missions 5, 7 and 8, available freely on the web site of the United States Geological Survey – USGS. To complete the scientific objective focused on the impact of heat waves on SUHI, both base images (collected during heat waves) and control images (collected in days without heat waves) were used.

4.1.2 Instruments

Concerning the instruments of the research, in order to complete the direct measurements, two portable meteorological stations produced by Davis Instruments company (Vantage Pro2™ model) were employed, along with nine mercury thermometers from the Meteorology Laboratory of the Faculty of Geography and three high-precision (0,3 °C) thermo-hygrometers Dostmann P400. To obtain a higher precision for both fixed and profile points, the temperature was measured using

portable meteorological shelters from cardboard. The geographical location of the points was recorded using the *GPS logger for Android* app.

4.2 Research methodology

4.2.1 AUHI evaluation through direct measurements

4.2.1.1 Data collection

The present study implied performing measurements in the urban canopy layer, at 1.5 meters from ground level. For AUHI evaluation, a mixed method was used, combining measurements in fixed points with mobile transverses. When compared to the classical method of fixed points, the advantage of this approach consists foremost in the reduction of costs, by using a limited amount of devices. One of the main limits of profile measurements is their incapacity to record simultaneously the temperature in different locations (Gartland 2008). To compensate for this disadvantage, in the case of mobile transverses, the deviation compared to the reference point has been used and not the absolute temperature from the moment of the measurement.

Regarding the altitude for performing the measurements, in the literature the vast majority of such studies (urban canopy layer heat islands) use as reference the value of 1.5 meters from the ground (Gartland 2008). Therefore, all the efforts to highlight the heat island in Cluj-Napoca city have taken into consideration the reccomended height.

Over the entire period temperature values were collected from the 9 fixed points as well. The recording interval for the points inside the urban area and the reference one outside it was five minutes. During the 24 hour measurements from May 13-14, 2015, the temperature was collected only every 10 minutes. The fixed points were chosen to reflect as good as possible the temperature differences from the local climate zones (LCZ) (Stewart and Oke 2012) and the reference point.

For the evaluation of AUHI in Cluj-Napoca city, the temperature measurements took place in different synoptic conditions that allow the manifestation of the phenomenon. This approach was used in order to minimize the risk to mistake the heat island generated by the city as a climatogenetic factor with an extra heat induced by topoclimatic differences or air mass advection (Lowry 1977). To highlight the manner in which the city influences the air temperature, it is very important to correlate the thermal profiles with altitude data (applying corrections). The heat island refers to an urban-rural temperature difference obtained at a similar elevation.

4.2.1.2 Data processing

The data collection phase was followed by the data processing one where corrections were applied to the raw data. In a first phase, altitude corrections were applied, for both fixed and profile points. Normally, this operation should be based on airsounding data, but, since such information is not available for the city's meteorological station from November 2012, the altitude corrections were based on the the average vertical thermal gradient (8).

$$T_{Xcor} = T_X + \frac{\Delta H}{100} \times 0.65 \quad (8)$$

T_{Xcor} = temperature corrected in point B, located in the urban area (°C);

T_X = temperature measured in point B, located in the urban area (°C);

$$\Delta H = H_X - H_R \quad (9)$$

ΔH= altitude difference between the observation and reference point (m);

H_X = altitude of the point that requires altitude correction (m);

H_R = altitude of the reference point (A), located in the nearby rural area (m);

0.65 = vertical thermal gradient (at 100 m) (°C).

For the temperature values collected in the fixed points only altitude corrections were necessary. On the profile ones, time corrections were also needed. In the next phase, the difference compared to the nearby rural area reference point was calculated for all the points. The "primary" deviation was obtained as a temperature difference from the measurement point in the urban area and the reference point outside it. The final deviation resulted by adding the altitude and, if necessary, the time corrections. If the temperature was recorded simultaneously in both the profile and the reference point, then, the final deviation was obtained with (10).

$$D = T_{PX} - T_R \quad (10)$$

D – the difference to be calculated for point X (profile point) (°C);

T_{PX} – the temperature measured in point (X) on the profile at the moment t_X (°C);

T_R – the temperature measured in the reference point at the moment t_X (°C);

t_x – the time when the temperature was recorded in point X on the profile (hour, minutes, seconds)

The time correction was computed only in the case of those profile points where the recording time was different from the measurement time in the reference point. Since the temperature in the fixed points was collected every five minutes, in some situations the profile

measurement was made between two recordings at the reference point. In this case, the proper value from the RP resulted by adding a time correction using the formula (11)

$$C_t = (t_2\text{-}t_1)/n \times d \quad (11)$$

C_t – time correction to be added to the temperature in RP (°C);

t_1 – the temperature measured in the reference point before the measurement on the profile point (°C);

t_2 – temperature measured in the reference point after the measurement on the profile point (°C);

n – the difference between the two consecutive measurements in RP (minutes);

d – difference between the measurement in the profile point and the previous measurement from RP (minutes);

After applying the time correction on the RP temperature, the deviation of the profile point was applied using (10);

Every correction needs to be added to the measured value before computing the difference between the point in the urban area and the RP.

4.2.2 SUHI evaluation and the impact of heat waves on LST

The intensity and spatial extent of SUHI was analyzed using the land surface temperature (LST), a defining parameter for the urban climate and a main indicator of SUHI. To quantify the influence of heat waves on SUHI, the LST deviation values for 18 city pixels have been extracted (same as the profile points) and also the reference pixel, containing the RP from Florești village. A part of the observation points from the direct measurements on AA' profile have been used. For every image captured during a heat wave in the summer of 2015, 3-4 control images have been chosen, acquired with the use of satellites in similar conditions from previous years (Herbel *et al.* 2017).

LST was obtained by integrating a set of equations into a model created in ArcMap 10.2 software, for both base images and control ones. The algorithm was different depending on the satellite scene. Thus, for Landsat 5 TM and Landsat 7 ETM+ imagery from the control group, the surface temperature was calculated according to the procedure presented by Imbroane *et al.* (2014). For Landsat OLI_TIRS scenes (base and control images), the method of obtaining LST is the one presented by (Herbel *et al.* 2017).

The creation of the application for LST retrieval from Landsat 8 OLI_TIRS consisted in covering 3 phases, according to the recommendations offered by Imbroane (2018): data analysis, projection and implementation. The processing of the satellite image data was made with the use of ArcMap 10.2 software and the calculations of the weight from the total surface, specific to every class (percent) was executed using Microsoft Excel 2007 software.

4.2.2.2 Projection phase

The projection phase included 2 components: data projection and the actual projection of the application. The first sub-phase implied the definitive and detailed establishment of the conceptual model, as well as the satellite imagery used inside the application and the operations to be performed on them. In the actual projection sub-phase, the entries were identified, as well as the type of operations for completing the scientific objectives and their order.

Below will be presented the equations integrated in the conceptual model, as they were described and applied by Herbel *et al* (2017). The first operation from the projection phase was computing the normalized difference vegetation index (NDVI), used to obtained the emissivity of the study surface. The NDVI map required the spectral reflectance bands in the red and near infrared domains (12):

$$\mathrm{NDVI} = (\mathrm{B5\text{-}B4})/(\mathrm{B5+B4}) \qquad (12)$$

Where:

B4 – Band 4 (red) of Landsat 8 OLI sensor

B5 – Band 5 (infrared) of Landsat 8 OLI sensor

The TIRS sensor of Landsat platform captures the spectral response of objects from the Earth's surface and stores it as digital numbers (DN) that can be converted in top of atmosphere radiance (TOA) with the use of the additive and multiplicative factors listed in the metadata file of the satellite scene. The TOA spectral radiance was obtained by scaling the digital numbers of TIRS-1 (Band 10), using the equation presented in the Landsat 8 User Manual (" Landsat 8 User Manual V 2.0" 2016, 60):

$$L_\lambda = M_L Q_{cal} + A_L \qquad (13)$$

Where:

L_λ – TOA spectral radiance measured by the instrument in Watts/ (m^2 * srad * μm)

M_L – Multiplicative scaling factor from metadata file

A_L – Additive scaling factor from metadata file

Q_{cal} – Calibrated digital numbers (DNs)

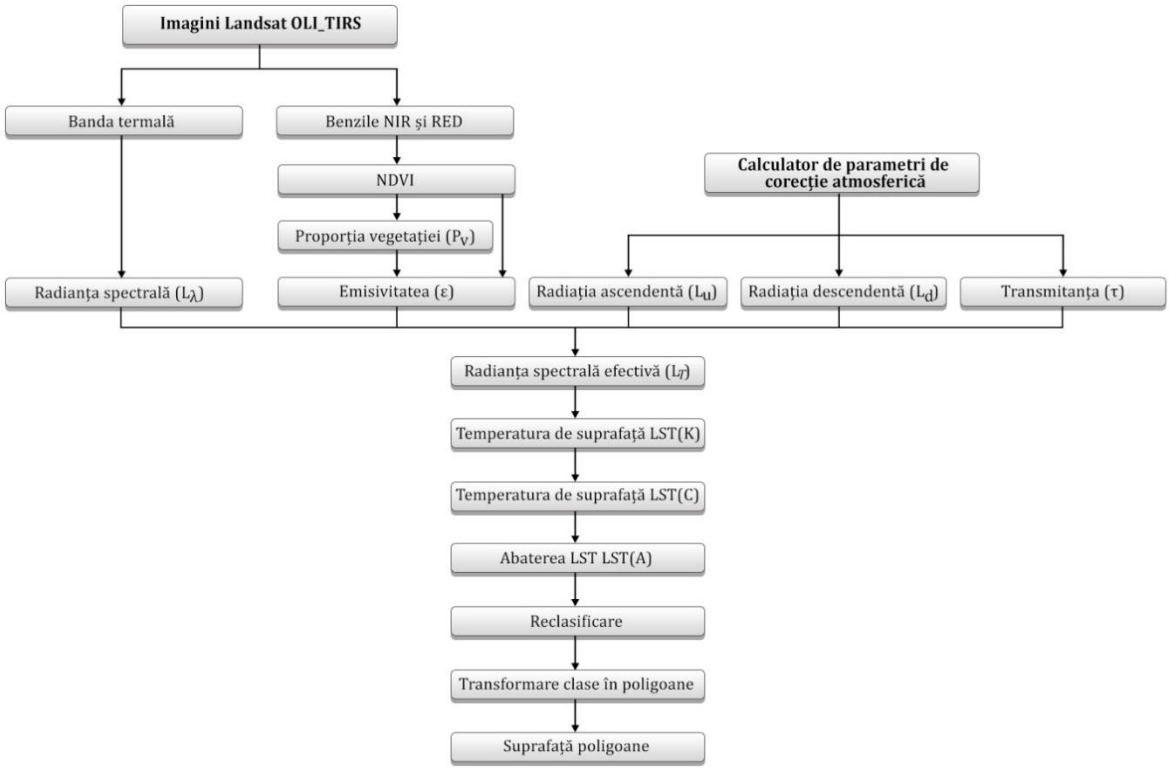

Figure 4.3 The conceptual model of SUHI evaluation in Cluj-Napoca city

The signal emitted by the terrestrial objects can be attenuated or accentuated by the atmosphere (Barsi *et al.* 2005). The TOA spectral radiance that reaches in space is capitated by the satellite sensor represents an association between three factions of energy: the radiation emitted from the Earth's surface, the upwelling radiation from the atmosphere and the downwelling radiation from space (Weng *et al.* 2004b). Therefore, the TOA spectral radiance measured by the instrument required corrections for atmospheric effects. In doing so, an online platform to generate the atmospheric correction parameters was used (available at http://atmcorr.gsfc.nasa.gov). Developed by Barsi *et al.* (2005), it integrates the radiative transfer code MODTRAN. The correction parameters were generated based on the profiles from the upper side of the atmosphere specific for mid-latitude cities during the summer, based on the spectral response curve of band 10 (Landsat 8) and surface conditions obtained by the local meteorological station at the time that the satellite traversed the study area.

Knowing these parameters allowed computing the actual radiation leaving from the Earth's surface, based on the method indicated by Yuan and Bauer (2007):

$$L_T = [L_\lambda - L_u - \tau(1-\varepsilon)L_d]/\tau\varepsilon \quad (14)$$

Where:

L_T – The actual radiation leaving the Earth's surface

L_λ – TOA spectral radiance measured by the TIR sensor (that reaches in space)

L_u – Upwelling radiation from the atmosphere

L_d – Down welling radiation from space

τ– Atmospheric transmission

ε –The emissivity of terrestrial objects

The emissivity values of terrestrial objects were necessary in order to scale the radiance of the blackbody. To identify these values, the NDVI threshold method proposed by Xiong *et al.* (2012) was employed:

(a) When NDVI < 0,05, ε = 0,973, but for water bodies, ε = 0,995;

(b) When NDVI > 0,70, ε = 0,99;

(c) When 0,05 ≤ NDVI ≤ 0,70, ε is calculated with (15 and 16).

When NDVI values were between 0,05 and 0,7, the vegetation proportion was calculated with (8), equation developed by Carlson and Ripley (1997). The final emissivity raster was obtained by applying (16), method created by Sobrino *et al.* (2004).

$$Pv = [(\mathrm{NDVI} - \mathrm{NDVI}_{min})/(\mathrm{NDVI}_{max} - \mathrm{NDVI}_{min})]^2 \quad (15)$$

Where:

Pv – Vegetation proportion

NDVI_{min} –NDVI value for bare soil

NDVI_{max} –NDVI value for pixels completely covered by

$$\varepsilon = 0.004Pv + 0.986 \quad (16)$$

Where:

ε – Emissivity values of pixels

Pv – Vegetation proportion (15)

After obtaining the spectral radiance from the Earth's surface, its temperature can be calculated with (17) based on Planck's law, adapted for Landsat 8 after the formula introduced by Chander and Markham (2003):

$$LST(K) = \frac{K_2}{\ln\ (K_1/L_T + 1)} \quad (17)$$

Where:

LST(K) – Land surface temperature (in Kelvin);

L_T - Spectral radiance from the Earth's surface (14);

K_1, K_2 –calibration constants for TIRS-1 (band 10); K_1= 774.88 watts/(m^2*ster*µm) and K_2 = 1321.07 K.

Since the temperature from 17 is expressed in Kelvin, the last phase of the algorithm for LST retrieval is the conversion to Celsius degrees (18):

$$LST(C) = LST(K) - 273.15 \quad (18)$$

Exploring the island intensity meant in a first step to calculate the LST deviation from the reference point in Florești for all the images using the *Raster calculator* tool from ArcMap software based on (19).

$$LST(A)_i = LST(C)_i - LST(C)_r \quad (19)$$

Where:

$LST(A)_i$ – The surface temperature deviation of pixel *i* from reference pixel, the same used in the direct measurements;

$LST(C)_i$ – Surface temperature of pixel *i*;

$LST(C)_r$ – Surface temperature of pixel r that contains the extra-urban reference point;

4.2.2.3 Implementation of the application

In this phase the items established in the projection phase were implemented: data introduction and activation of the commands according to the conceptual model. The activation of the commands has as result the generation of new maps based on the existent ones. The command sequence was executed according to the algorithm chosen in the previous step. The images of LST deviation were reclassified using the *Reclassify* tool in 7 classes of temperature: (°C): <25, 25.1-30, 30.1-35, 35.1-40, 40.1-45, 45.1-50, >50. Afterwards, the reclassified raster images were converted to polygons. In the attribute table, the surface of every class was calculated as well (*Calculate geometry*). The percent from the total surface of every class for each of the three images from the

summer of 2015 were obtained in Microsoft Excel software, based on the values in the attribute table of the .shp file (Herbel *et al.* 2017).

4.2.3 Heat wave identification

The identification of the heat waves that affected the study area in the summer of 2015 was performed according to the percentile method based on relative thresholds, using the maximum daily temperature recorded at the local meteorological station. The 90 (P90), 95 (P95) and 98 (P98) percentiles were calculated for every day of the year using the PERCENTILE function integrated in Microsoft Excel (v 2007) software. The maximum temperature (T_{max}) of every day from the summer of 2015 was compared to P90, P95 and P98 values for those days of the year. Afterwards, only the days when the maximum temperatures were higher than the values of the chosen percentiles were selected. In the next phase, we selected as heat waves the periods with 3 consecutive days when the percentiles were exceeded. The intensity of the values was considered moderate for the days when T_{max} exceeded P90, severe when T_{max} exceeded P95 and extremely severe when T_{max} exceeded P98 (Croitoru 2014, Croitoru *et al.* 2018).

5. RESULTS AND DISCUSSIONS: UHI CHARACTERISTICS IN CLUJ-NAPOCA CITY

The results of the direct measurements

Summary of the fixed points results

The analysis of the data collected from the fixed points during the seven measurement campaigns allowed the identification of the local climate zones and the characteristics of the urban tissue favorable for the development of UHI and also of the ones that neutralize it. The observations have facilitated the exploration of UHI depending on the season, the amplitude of the deviation and their tendency in the relative thermal stability interval.

The highest differences compared to the extra-urban RP were observed the high and medium height compact types (Table 5.5).

The identification of the maximum values in other fixed points from other local climate zones is due to special circumstances like the extremely severe heat wave that started in August, 5 2015 or to other meteorological phenomena different than UHI.

Table 5.1 Temperature deviation to RP, with time and altitude corrections, in fixed points (°C)

	SPRING						SUMMER						AUTUMN						WINTER		
	9-10 May 2015			13-14 May 2015			22-23 July 2015			7-8 August 2015			24-25 October 2015			29-30 October 2015			22-23 February 2016		
	AVG	MIN	MAX	AVG	MIN	MAX	AVG	MIN	MAX	AVG	MIN	MAX	AVG	MIN	MAX	AVG	MIN	MAX	AVG	MIN	MAX
PF1–compact, high-rise	-	-	-	**1.9**	0.9	3.0	**3.2**	2.8	3.8	**3.1**	2.8	3.6	**1.5**	1.1	2.3	**1.5**	0.3	2.6	**0.6**	-0.1	1.6
PF2 – compact, High-rise	-	-	-	**1.5**	0.5	2.3	**2.6**	1.5	3.3	**2.5**	1.9	3.3	**1.2**	0.8	1.6	**0.6**	-0.6	1.7	**1.0**	0.1	2.6
PF3 – compact, midrise	**1.9**	1.1	2.9	**2.1**	0.9	3.0	**2.8**	2.5	3.1	**2.5**	2.1	3.1	**1.3**	0.8	2.0	**0.9**	-0.3	2.1	**0.1**	-0.7	2.3
PF4 – compact, low-rise	**1.6**	0.6	2.6	**1.4**	0.8	2.0	**2.6**	1.8	3.0	**2.7**	2.2	3.2	**1.3**	0.7	2.3	**1.4**	0.1	2.6	**1.5**	0.6	2.0
PF5 – open, low-rise	-	-	-	**1.5**	0.5	2.5	**2.8**	2.3	3.2	**3.5**	3.0	4.1	**1.4**	0.6	2.2	**0.9**	-0.6	2.1	**0.3**	-0.8	1.1
PF6–water; large low-rise	-	-	-	**-0.1**	-1.1	0.8	**0.1**	-0.4	0.6	**0.3**	-0.4	1.2	**0.4**	-0.2	1.0	**-1.1**	-2.5	0.3	**-0.6**	-1.3	1.3
PF7 – scattered trees	**0.9**	0.6	1.2	**1.2**	0.1	2.6	**2.7**	2.4	3.1	**3.2**	2.7	3.7	**1.3**	0.4	2.1	**1.2**	-0.3	2.4	**0.6**	-0.4	1.4
PF8 – sparsely built	**-0.8**	-0.7	-1.8	**0.4**	-0.5	1.8	**0.6**	0.0	1.0	**0.9**	0.6	1.3	**-1.0**	-1.6	0.5	**0.1**	-1.8	1.1	**3.1**	1.1	5.5

On August 7, 2015 the maximum difference was observed in the open low-rise type (observation point 5 - residential area from Andrei Mureșanu district). In February 22-23, 2016 warm air mass advection was detected in the sparsely built type (observation point 8 – the local

meteorological station from Gruia district). High differences were noticed in these situations, up to 5.5 °C compared to RP.

The lowest values of the temperature deviations were observed in the vast majority of cases on the shore of Someșul Mic river. The average temperature in the second autumn campaign (October 29, 2015) was up to 1.1 °C lower than the one from the reference point. In the rest of the data sets (May 9-10 and October 24-25), the minimum deviation corresponded to the observation point from the local meteorological station (sparsely built local climate zone).

Concerning the seasonal variability of UHI, the maximum intensity was noticed during the summer measurements, followed by the spring and autumn ones. The data collected during the winter are insufficient for such a generalization.

An analysis of the temperature graphics created based on the 5/10 minutes consecutive observations for each of the observation points indicate as well that the heat island is the most intense during the summer for the vast majority of the situations.

The values were recorded on the shore of Someșul Mic river. The small or even negative differences to RP are found here because of the microclimate particularities, and more precisely, to the evaporation and the heat transfer that occur at the interface between the two environments. All these lead to a smaller value of the air temperature. In the urban environment, the water of the rivers and the particles in suspension free the heat gathered inside the city downstream from the absorption point. This mechanism, along with the processes presented above, explain both the reduced temperatures in observation point 6 and the neutralization of UHI.

Ranking the values based on the season is also difficult for the observation point in the sparsely built type from Gruia district. This situation is due to the altitude difference and the characteristics of the urban tissue nearby the point (low building density and abundant vegetation). If the other fixed points are located between 336 and 383 meters above sea level, the altitude of the local meteorological station is 410 m. These particularities of the observation points 6 and 8 generate temperature values comparable to the ones from RP and indicate the efficient patterns to mitigate the UHI effect.

The differences to RP is of approximately 4°C for all the data sets from all the points, except OP8 in the February 22-23, 2016 campaign when extreme deviations up to 5.5 °C were noticed, raising the thermal amplitude of the values as well.

In the fixed points from the local climate zones favorable to UHI development, the deviation to RP is relatively constant during the relative thermal stability interval in both of the summer campaigns and a little bit during the winter too. The difference to PR tends to increase during the autumn measurements and to decrease during the spring ones. Even so, the lack of data is insufficient to draw definitive conclusions concerning these tendencies.

Summary of the thermal profiles results

a. AA' profile

The UHI effect was observed in all data sets, but the thermal graphic was different in every case, as a dome (during summer and winter measurements) or concave. The differences are related to the synoptic conditions and the local air movement, specific to every campaign. The ***shape*** of the island is well defined, especially during the summer. The presence of intense heat waves determines the expansion of the heat islands to the east and the strong heating of the first half of the profile. This part corresponds to Someșeni district, a former sub-urban locality that was assimilated by the city. At the end of the autumn and winter, the phenomenon is more intense in the second half of the profile, the western part of the city respectively.

The airport area is a local *hot-spot*, always warmer than the surroundings. This fact is is related to the intense urbanization from in the last years, determined by the intensification of the road and air traffic. Building residential and industrial constructions in the nearby area also contributed to this process. The local variations on the profile are caused by micro-advection and also by the modification of the urban tissue along the route.

The ***maximum intensity*** was signaled during the summer, with differences to RP up to 4.3°C. In the data sets from other seasons, the maximum deviation ranged between 2.0 and 2.6°C. In the vast majority of the data sets, Mărăști district was warmer because of the urban tissue characteristics, higher construction density and height regime but also to lower altitude (the district is located on the second terrace of Someșul Mic river). During heat waves, the deviation increases proportionally with the urbanization degree, while the surfaces with more vegetation remain cooler.

The maximum ***thermal amplitude*** was recorded during the extremely severe heat wave from august, but at the end of autumn as well. This was probably due to the anthropogenic heat from heating installations. The ***average deviation on profile*** had the maximum value, as well, at the beginning of August – 2.9°C.

The ***minimum intensity*** of the island on AA' profile was observed at the end of October, when the temperature from observation point 5 was 1.6°C lower than the one from the reference point. Generally, the negative deviations appeared in observation points located in the vicinity of water bodies or areas cover by vegetation. The reasons are the different cooling rate and micro-advection, especially during cold weather. Negative deviations were noticed at the end of autumn and winter, but in the first spring measurement as well.

b. BB' profile

On the second profile, UHI is visible in every one of the analyzed situations. The ***shape*** is different in every one of the campaigns, but well defined.

The maximum intensity area starts from the city center and moved a bit towards south-east, where the urban tissue alternates between residential areas of houses with low height regime and apartment buildings with four floors. The highest temperature values were usually recorded in this segment of the profile (Constantin Brâncuși street) and less in central part of the city.

The ***maximum intensity*** was recorded in the summer, during the extremely severe heat wave, with a difference up to 3.6°C to RP. In the other measurement campaigns, the maximum intensity is variable, ranging from 1.6 (May 13-14, 2015) to 3.0°C (during the first summer measurement and at the end of autumn). It is known that UHI can be more prominent during cold weather, because of the anthropogenic heat contribution.

Based on the analyzed data and the results reported in the literature, we can conclude that in Cluj-Napoca city, the intensity of heat waves influences the intensity of the island as well. This reflects also in the average profile deviation values, 0.8°C higher during the extremely severe heat wave, compared to the moderate one (1.8°C in August 7-8, as opposite to 1.0°C in July 22-23).

The ***minimum intensity*** was usually noticed at the beginning of the profile, in the segment covering Baciu village. The first autumn campaign is an exception, because the minimum deviation was detected in a green area near Grand Hotel Napoca, on the shore of Someșul Mic river, where the air temperature was identical to the one from RP. This demonstrates the modulating effect of vegetation and water bodies on the air temperature. The minimum intensity was usually very close to 0 because of the intense urbanization of Florești (the location of RP) in the recent years. The low house prices and terrains lead to a massive migration from Cluj-Napoca, especially of the younger population, affecting the air temperature patterns as well. The highest negative deviation, of -4.2°C was identified in the second autumn campaign, when the weather suddenly got colder. The drop of

daily average temperatures has induced an increase of the thermal amplitude up to 7.2°C. This value is one of the largest signaled in the entire period, determined probably by the local circulation and by the different cooling rate in Baciu village.

The topography of the terrain and, more precisely, the increase of altitude towards the Apahida-Vâlcele bypass lead to ***thermal inversions*** in 5 from the 7 measurement campaigns. In some situations, the highest value was identified at the end of the profile, but this cannot be attributed to UHI. In the graphic from February 2016, a 3.2°C thermal inversion induced deviation to RP was observed in this segment of the profile.

c. CC' profile

As it was mentioned before, the CC' profile is the least representative, with altitude values ranging from 331 to 711m. This feature determines the frequent apparition of thermal inversions at the end of the profile. The phenomenon was noticed in all data sets, except the ones from May 9-10 and October 24-25. In this last set, the sudden increase of altitude from the end of the profile can be a result of thermal inversion or caused by the modification of the urban tissue and the increase of anthropogenic heat levels compared to the previous observation point.

The typical, convex, island ***shape***, can be observed only in the first part of the profile, up to the central part of the city. The occurrence of thermal inversion influenced the thermal amplitude, generating extreme values for this parameter, especially during cold weather (7.2°C in October, 29-30 and 7.8°C in February 22-23).

If we consider only the data from the first part of the profile, where the deviation values reflect the presence of UHI, the ***maximum intensity*** of the heat island is specific to the city center and the effect is more pronounced during the summer. The maximum 5.6°C deviation to RP observed at the entrance in Feleacu village in February 22-23, 2016 is a result of thermal inversion and not of the heat island phenomenon.

The highest value of the ***average profile deviation*** was 1.9°C, being recorded during the extremely severe heat wave from the beginning of August, 2015.

The ***minimum intensity*** was identified at the beginning of the profile, on Valea Chintăului and Oașului Street. The values reached the lowest threshold of -3.3°C during the campaign conducted in May 9-10, 2015.

5.2 The surface urban heat island (SUHI). Heat wave impact on SUHI.

The occurrence of heat waves during the summer on the territory of our country is related to warm air mass advection from South or South-east associated to high pressure systems, originating from the north of Africa or from Azore Islands (Sfîcă et al. 2017). As shown in the literature review chapter, there is enough evidence that indicate a mutual amplification relation between UHI and heat waves. In these circumstances, the exploration of SUHI during extreme events was attempted. The research was focused on three different events that affected the study area in the summer of 2015 in order to explore its maximum intensity.

5.2.5 Summary of the results from the satellite image data analysis

SUHI was explored during three episodes with extreme temperatures. The phenomenon was observed in every situation, with LST deviations to PR that exceeded 5°C. As expected, the lowest values were encountered in the areas covered by forests, green spaces and water bodies, and the highest in industrial and commercial areas, in the city center, as well as in densely built districts. Even if the urban tissue from the Eastern part of the city is very similar to the one from the Western part (Mărăști and Mănăștur districts), SUHI is asymmetrical, more intense in the eastern part of the city for all the analyzed cases. The mountain breeze, dominant in the west and south-west, combined during the day with SV micro-advection towards the city of the cold air from the forest that displaces the warm air to the western districts, seem to be the main factors explaining the asymmetry of Landsat 8 retrieved SUHI. For the entire area taken into consideration, the shape of SUHI was the same, but the intensity seems to be influenced by the intensity of the heat wave.

For the extremely severe heat wave, an intensification of SUHI occurred, especially in the central area and in the eastern side. During the severe heat wave, SUHI intensity is similar to the one recorded in the control images, in normal conditions, without extreme thermal events. In this same situation, the heating of the agricultural land determined the expansion of SUHI that included the bare land surrounding the urbanized surface.

Because of the low number of satellite images, these preliminary conclusions should be treated with precaution. It is recommended that extra research should be done on the topic in the following years, that contain a larger number of case studies during extreme heat events.

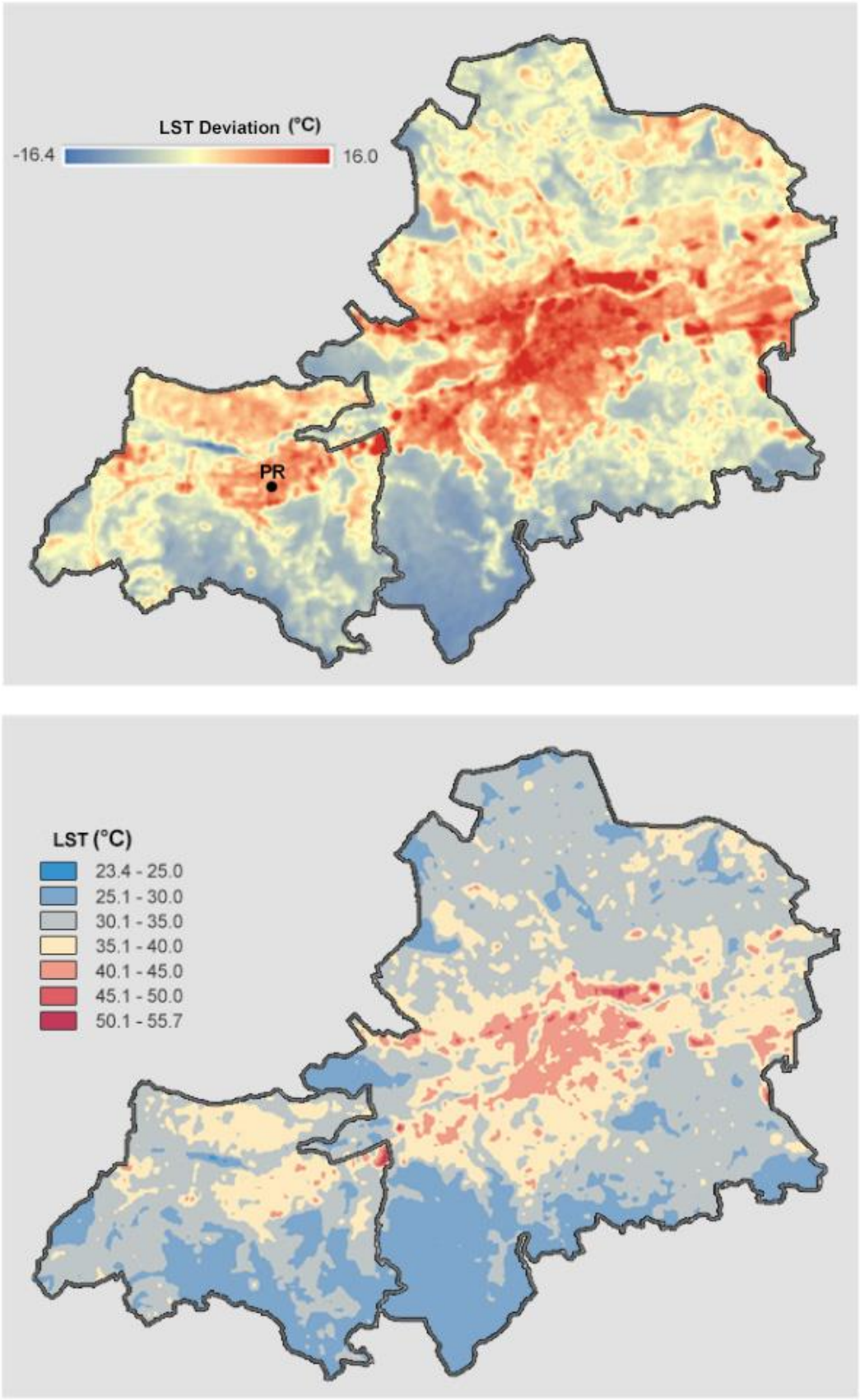

Figure 5.1 The temperature deviation to the reference point in Florești village (top) and LST classes (bottom) in July 7, 2015, 11:40 GMT after Herbel *et al.* (2017)

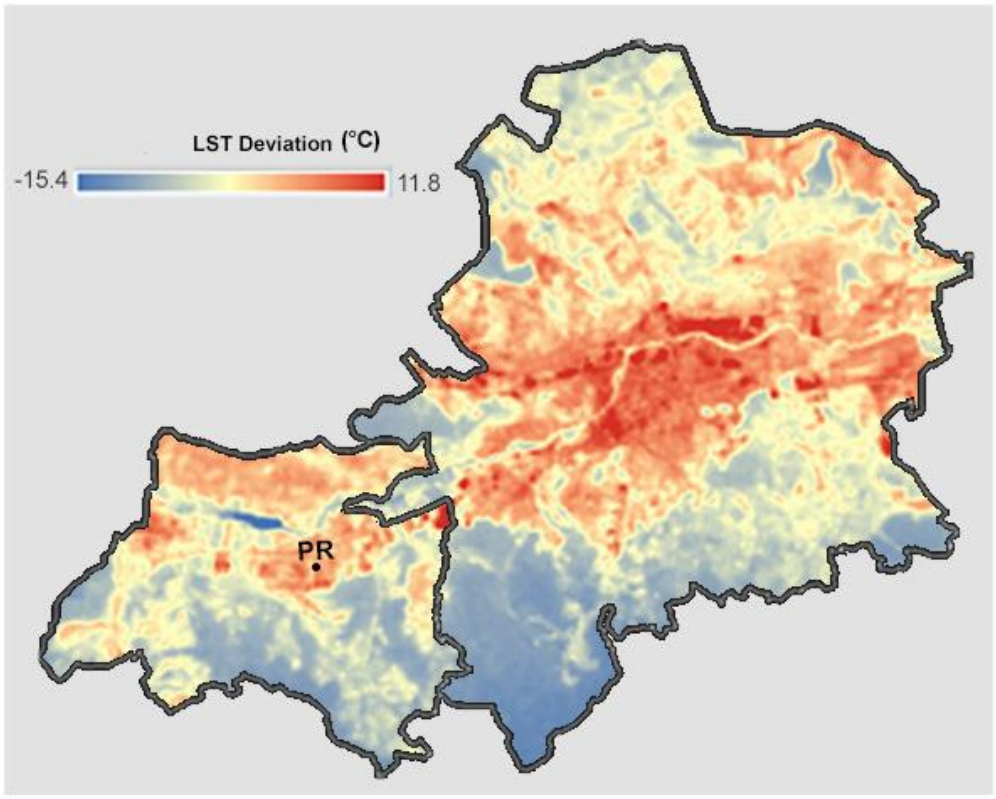

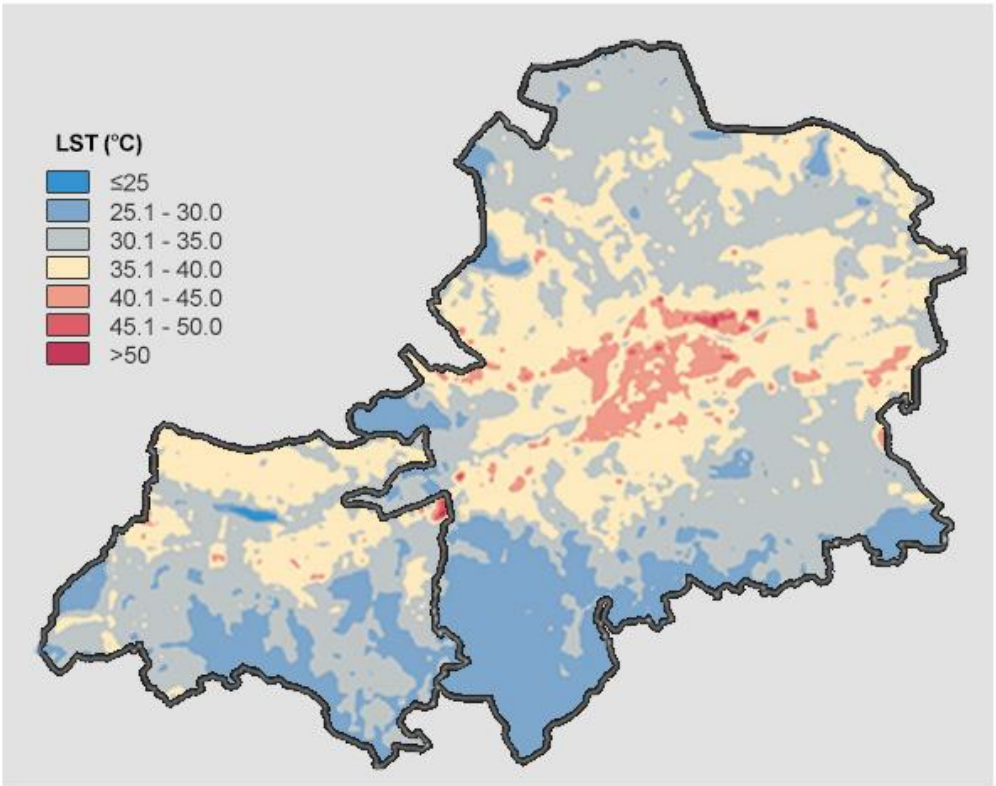

Figure 5.2 The temperature deviation to the reference point in Florești village (top) and LST classes (bottom) in July 23, 2015, 11:40 GMT after Herbel *et al.* (2017)

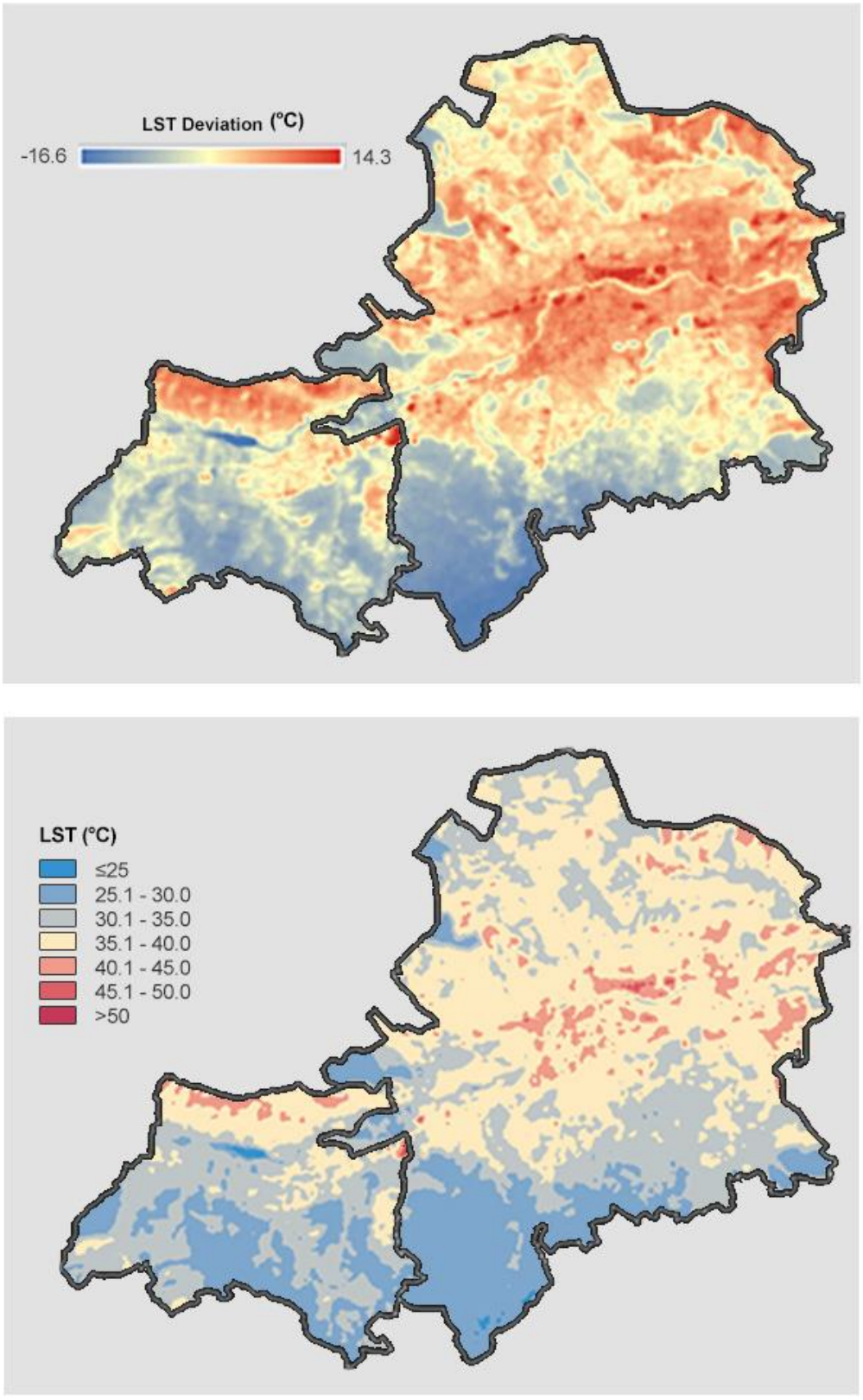

Figure 5.3 The temperature deviation to the reference point in Florești village (top) and LST classes (bottom) in August 8, 2015, 11:40 GMT after Herbel *et al.* (2017)

5.2.4 The impact of heat waves on the surface temperature

To identify how heat events influence the SUHI intensity, the LST deviation values of 18 pixels were extracted, as well as the value of the reference pixel from Florești village. The points are identical to the ones used for the direct measurements on AA' profile that traverses the city from E to W.

For every image captured during a heat wave from the summer of 2015 a couple of control images were chosen, from days without extreme thermal events. These were collected in similar periods from the previous years and processed in previous research efforts of SUHI evaluation (Herbel 2013; Imbroane *et al.* 2014).

Even if the analyzed pixels were located along the street network, on the route some significant differences to RP were observed, up to 5.5°C (Figure 5.43).

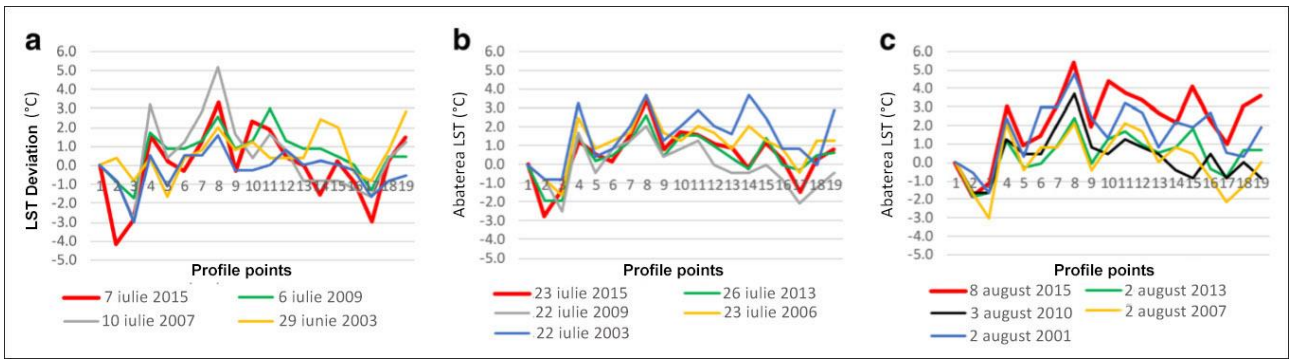

Figure 5.4 LST deviation calculated for the profile points on the E-W route (Airport-Florești), at the beginning of July (a), at the end of July (b) and at the beginning of August (c) after Herbel *et al*., 2017)

The surface temperature analysis of the 18 points, for both base (the ones from the summer of 2015) and control images, indicate that the SUHI intensity increases with the intensity of the heat wave and appears to be influenced by the extremely severe ones. In this last case, the deviations values to RP exceeded 5.0°C in the city center (point 8). The LST patterns were similar for all the situations considered, but the intensity was different from one situation to another (Herbel *et al*. 2017).

In the case of the extremely severe heat wave, the deviation values to RP were the highest, for both the base and the control groups. The deviations from the first two heat waves have average values compared to the other observed values. In this situation, we can conclude based on existing data that extremely severe heat waves determine the intensification of SUHI, while the moderate/severe ones have a much smaller influence. Additional research is needed to establish a clear conclusion regarding this aspect (Herbel *et al*. 2017).

6. UHI MITIGATION. POSSIBLE SOLUTIONS FOR CLUJ-NAPOCA.

If by 2011 observations of UHI in over 200 cities all over the world were reported in the entire world, in the last years, the urban climate studies are focused more on UHI mitigation rather than evaluation. The objective of the present chapter is to identify in the literature sustainable solutions and practices to diminish the effects of development on the urban climate, but also results obtained after their implementation in different locations. This step represents a *sine qua non* condition to formulate a UHI mitigation strategy in Cluj-Napoca city, where the maximum identified intensity exceeds 3.5°C.

6.1 UHI Mitigation. Current practices.

In the last years the concept of „Green infrastructure" is used ever more often. It can be defined as an ensemble of anthropic elements that confer multiple ecological functions at building level, but at an urban scale as well. From these functions, the reduction of energy consumption, ambient temperature and UHI mitigations are major priorities (Pérez et al. 2014).

For the mitigation of UHI and the reduction of the energy consumption, building level, district level, municipal or regional level strategies can be applied. At building level, the objective is to maintain a low temperature during the night, when the heat stored by the urban structures is released slowly. Next, a series of techniques with proven efficiency for reaching these goals will be presented.

6.1.1 Using adequate materials for buildings, pavements and rooftops in order to reduce their albedo value

The construction materials frequently found in the urban environment can be divided in three major categories: the ones for the building envelope, for pavements and rooftops.

6.1.1.1 Sustainable solutions for building envelope

Increasing the albedo of surfaces has a direct impact on the energy balance of constructions. In warm areas, the modification of the surface albedo is the most promising tool for the reduction of the air temperature, especially if we consider the initial and maintenance costs (Taha *et al.* 1988).

Using in the building envelope retro-reflective materials that reflect the incident radiation back on its original direction proved to be efficient in diminishing the cross radiation to the buildings and the street network (Akbari *et al.* 2016).

The current research is also focused on inserting phase change materials (PCM) or combinations between PCMs and reflective ones in the building envelope. Unlike sensitive traditional materials like stone or brick, PCMs store the heat in latent manner and can be up to 8.0°C colder than the normal ones of the same color (Karlessi *et al.* 2011).

6.1.1.2 Sustainable solutions for pavements

The pavements represent a significant part of the urban tissue, with a great input to the formation of UHI. The efficient mitigation of the phenomenon at this level, imposes the reduction of the sensible heat flux released by the pavements in the urban atmosphere and, implicitly, the reduction of their temperature. Modern materials and techniques for "cool" pavements are currently available (Santamouris 2013).

The *reflective pavements* combine surfaces with a higher albedo and thermal emissivity. From the techniques used for the increase of the albedo we mention using additives like slag cement and fly ash; applying white paint (aluminum, calcium hydroxide or acrylic elastomeric paint based); applying (color) paint, reflective in IR domain, using reflective and colorless binding agents, resin pavements etc.

The porous or permeable pavements, with or without vegetation, constitute examples of "cool" pavements. The ones without vegetation are based on a pore or hole system that allows the water circulation. They usually have a lower albedo than the impervious ones and imply more intense convective fluxes to the atmosphere. From these we mention the porous/rubberized asphalt, interconnected concrete pavements or concrete/plastic grids filled with gravel (Figure 6.1). The pervious pavements with vegetation ensure cooling by evapotranspiration. These include cellular pavements with grass, reinforced grass and networks of pavements that allow the grass to grow in between.

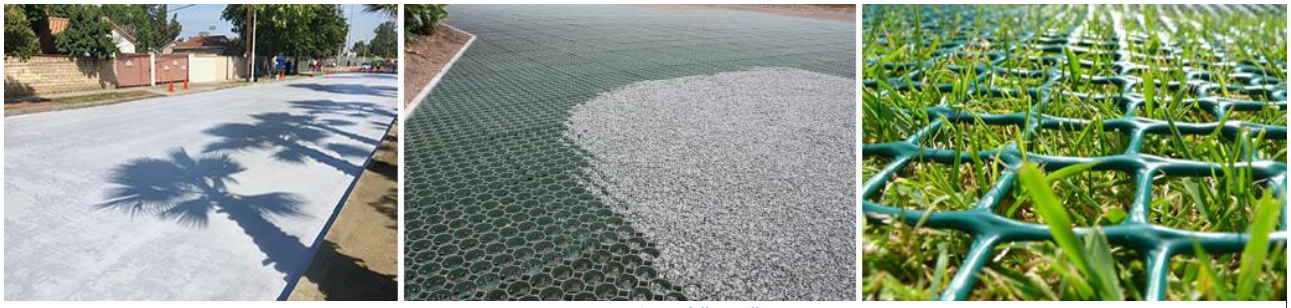

Figure 6.1 Some examples of "cool" pavements.
Sources: www.lonelyplanetwpnews.imgix.net; www.terram.com.au; www.amazon.co.uk

Reducing the temperature of pavements can be achieved using mechanical systems and more precisely, circulating a fluid or even the underground water in the mass of the pavement to eliminate the heat excess.

Using phase change materials (PCMs) for pavements contributes to the diminution of the convective flux towards the atmospheric air, decreasing the heat island effect (Karlessi *et al.* 2011).

Shading the paved areas determines, as well, the substantial reduction of their temperature. Shade can generated be by artificial means, or with natural solutions like shade trees and green pergolas.

6.1.1.3 Sustainable solutions for roofs

Roofs generally represent 20 to 30% of the urban surface (Susca *et al.* 2011). Their rehabilitation or conversion to green spaces can have a positive impact, both at city and building level.

Cool roofs reduce the heat input and the amount of energy spent on AC systems, contribute to increasing the lifetime of the roof membrane, improve the efficiency of thermal and phonic insulation, reduce air pollution and the emission of greenhouse gasses and mitigate the UHI effect (Shahmohamadi *et al.* 2010). Depending on the technique used for mitigation, the cool roofs can be classified in *reflective* (when the objective is the increase of albedo value) and *green* (when vegetation is placed at roof level and the reduction of temperature occurs due to evapotranspiration). Both types of cool roofs contribute to the reduction of sensible heat flux to the atmosphere and, implicitly, to UHI mitigation.

6.1.2 Landscape design of spaces from the urban environment

Urban design plays a key role in mitigating UHI. Reintroducing green spaces in the cities can be achieved as urban forests (parks), squares, street alignments, green roofs or vegetal walls. The cooling potential of green spaces is well documented in the literature, for different latitudes. The presence of vegetation ensures a cooling effect of 1-4 °C, that propagates at 100-1000 m inside the urban area, but is highly dependent on the amount of water available for the plant (Kleerekoper *et al.* 2012).

In UHI mitigation, the shade of trees can have a significant impact, by reducing the amount of energy spent on cooling, the thermal convection rate inside the building and by diminishing the radiation exchange between the building wall and the sky. The efficiency of shading depends on the chosen specie and the shape of the canopy is more important than its density.

6.1.2.1 Vertical green spaces

In the absence of spaces available for creating parks and urban gardens, the vertical green spaces can constitute an alternative for UHI mitigation. The reduction of temperature occurs by two different means: the evapotranspiration and the shading of the building walls. Shading is frequently nominated as being the most significant aspect of the cooling effect of plants (ensured by intercepting the solar radiation), where the volume of the foliage plays a key role (Cameron *et al.* 2014). Green surfaces like vegetable walls, placed in certain parts of the building or even inside them offer natural ventilation, thermal and phonic insulation, can reduce the energy consumption and the urban-rural temperature difference (UHI impact).

In temperate zones, the temperature recorded in the nearby air volume of a green wall can be up to 3°C compared to a normal wall (Cameron *et al.* 2014). The efficiency of green walls in reducing the atmospheric air temperature depends, however, on many factors like the specie, the shape and vigor of the plant, the crown characteristics, humidity and seasonality.

Figure 6.2 Vertical garden designed by Patrick Blanc at Museum Quai De Branly, Paris.
Source: http://www.i.pinimg.com

6.1.2.2 Horizontal green spaces

Creating new parks and gardens in the urban environment represents a very difficult to accomplish desideratum because of the pressure of real estate market. In the absence of residual spaces that can be converted to green area, the green horizontal surfaces can be created at different

levels, not only on terrain level. Planting trees, creating green roofs, pervious vegetation pavements (briefly presented above) and replacing standard materials from parking lots with vegetation can constitute possible UHI mitigation techniques.

6.1.2.2.1 Shade trees and urban vegetation

Besides the decorative valence, shade trees in the urban environment intercept the solar radiation before this heats the building or pavement. They reduce the wind speed under their crown and protect buildings from the cold winter winds. Shade trees offers significant benefits by reducing the temperature of the atmospheric air, as well as by decreasing the need for AC systems (Akbari 2005).

6.1.2.2.2 Creating green roofs

Green roofs are partially or totally covered by vegetation placed in a growing environment and that has on its base an impervious membrane. Among the building level benefits of this UHI mitigation technique we can mention the lower energy consumption, higher phonic insulation level, increasing the durability of the roof materials and a superior ambient air from a qualitative point of view (Kolokotsa *et al.* 2013). Green roofs have a higher albedo than the dark materials usually encountered at this level, they contribute to the increase of pervious surfaces in the city and of the amount of water available for evapotranspiration.

6.1.2.2.3 Converting parking lots from urban areas to green spaces

The efficiency of converting parking lots to green spaces has proven to be small because of their low weight in the urban environment. Because the reduction of temperature as an effect of creating green spaces happens exponentially, the use of this method is recommended only in association with others, in an integrated UHI mitigation approach.

6.1.2.3 Cooling effect of water bodies

The presence of water bodies inside the city presents a high cooling potential, especially for flowing waters. Their role in the attenuation of the UHI effect is very well documented in the literature. The water has a cooling effect of 1 to 4 °C that propagates to approximate 30-35 m (Kleerekoper *et al.* 2012). The fluxes specific to flowing water can be reproduced by creating small size hydrotechnical structures (lakes, pools, ponds, tank, waterfalls) with a decorative and functional role, as well as for UHI mitigation.

6.1.3 Natural ventilation

The natural ventilation represents the most efficient technique of passive cooling that can ensure the temperature reduction of spaces during nighttime and daytime. From the techniques used to achieve passive cooling we can mention *the arrangement of windows perpendicular to the direction of the dominant wind* (this would offer a good ventilation and a qualitative interior climate), *using ventilated roofs* and the *variation of the height regime of buildings* to facilitate the movement of air.

6.2 General directions of a UHI mitigation strategy in Cluj-Napoca city

Even if there are significant associated costs, the formulation of a UHI and UHI effects mitigation strategy is required in Cluj-Napoca city, where the intensity of the heat island identified in the present paper exceeds 3.5°C during the summer.

Based on a close review of the literature, the implementation of an integrated strategy in Cluj-Napoca is demanded. This should include building and city measures, like the creation of new green spaces, increasing the urban reflectivity, implementing a set of good practices in the urban design and informing the population. These are indispensable methods for mitigating the heat islands effects and for the consolidation of a green infrastructure in Cluj-Napoca city. The absence of such a strategy affects the environment, the society and the economy and the negative effects are even more amplified during heat waves.

Figure 6.3 Traditional green facade, modular green walls and perimeter flowerpots;
Source: www.static1.squarespace.com; www.souceable.net; www.lksf.org

7. CONCLUSIONS

The present thesis was focused on the evaluation of AUHI, SUHI and the impact of heat waves on the surface temperature, as well as on identifying sustainable solutions for Cluj-Napoca, a first rank municipality and second largest city in Romania after the capital Bucharest.

For the evaluation of UHI in Cluj-Napoca, a mixed approach was used: measurements in fixed (stationary) points were associated with mobile transverses and the estimation of the surface temperature based on Landsat 8 image data.

AUHI was detected in all the measurement campaigns. In the fixed points, the highest differences to RP (hot-spots) were usually identified in the high and medium compact types – districts with apartment buildings and significant impervious areas, but in the city center as well. The lower height regime of the buildings from the 18^{th} and 19^{th} centuries determine lower air temperature in the central area compared to the collective living districts. The occurrence of the highest intensity in other local climate zones is related to other phenomena than UHI (heat waves, warm air mass advection, thermal inversions).

On the thermal profiles, the UHI effect was observed in every one of the seven data sets, but the thermal graphs presented different shapes. The differences are related to the characteristics of every profile, to the synoptic conditions and the local air circulation.

In the summer of 2015, the surface temperature was analyzed as well, based on three different satellite scenes captured by the OLI_TIRS sensor during three heat waves of different intensity.

SUHI was detected in all the analyzed cases, with temperature differences to RP of over 5°C. The highest values corresponded to industrial, commercial and residential areas, while the lowest to green spaces, water bodies and forest areas.

The most common solutions for UHI mitigation are the reintroduction of urban vegetation and increasing the albedo value of surfaces inside the city.

The present study was focused as well on identifying possible solutions for Cluj-Napoca city where the intensity of UHI exceeds 3.5°C. The main directions of an integrated strategy (building and city level) for UHI mitigation should include the creation of new green spaces, increasing the urban reflectivity, implementing a set of good practices in the urban design and informing the population.

SELECTED BIBLIOGRAPHY

Akbari, Hashem. 2005. "Energy Saving Potentials and Air Quality Benefits of Urban Heat IslandMitigation." *Lawrence Berkeley National Laboratory*, August.

Akbari, Hashem, Constantinos Cartalis, Denia Kolokotsa, Alberto Muscio, Anna Laura Pisello, Federico Rossi, Matheos Santamouris, Afroditi Synnefa, Nyuk Hien Wong, and Michele Zinzi. 2016. "Local Climate Change and Urban Heat Island Mitigation Techniques – the State of the Art." *Journal of Civil Engineering and Management* 22 (1): 1–16.

Barsi, Julia A., John R. Schott, Frank D. Palluconi, and Simon J. Hook. 2005. "Validation of a Web-Based Atmospheric Correction Tool for Single Thermal Band Instruments." In *Proc. SPIE 5882, Earth Observing Systems X, 58820E*, 5882:58820E-58820E – 7.

Belozerov, Valeriu. 1972. "Clima Orașului Cluj Și a Împrejurimilor - Teză de Doctorat."

Cameron, Ross W.F., Jane E. Taylor, and Martin R. Emmett. 2014. "What's 'Cool' in the World of Green Façades? How Plant Choice Influences the Cooling Properties of Green Walls." *Building and Environment* 73 (March): 198–207.

Carlson, Toby N., and David A. Ripley. 1997. "On the Relation between NDVI, Fractional Vegetation Cover, and Leaf Area Index." *Remote Sensing of Environment* 62 (3): 241–52.

Chander, G., and B. Markham. 2003. "Revised Landsat-5 TM Radiometric Calibration Procedures and Postcalibration Dynamic Ranges." *IEEE Transactions on Geoscience and Remote Sensing* 41 (11): 2674–77.

Cristea, Marius, Codruta Mare, Ciprian Moldovan, and Thomas Farole. 2017. *ORAȘE MAGNET - Migrație Și Navetism În România*. București: World Bank Group.

Croitoru, Adina Eliza. 2014. "Heat Waves. Concept, Definition and Methods Used to Detect." *Riscuri Și Catastrofe XIII* 15 (2).

Fărcaș, Ioan. 1999. *Clima Urbană*. Cluj-Napoca: Casa Cărții de Știință.

Gartland, Lisa. 2008. *Heat Islands: Understanding and Mitigating Heat in Urban Areas*. London ; Sterling, VA: Earthscan.

Grubler, Arnulf, Xuemei Bai, Thomas Buettner, Shobhakar Dhakal, David J. Fisk, Toshiaki Ichinose, James E. Keirstead, et al. 2012. "Urban Energy Systems." In *Global Energy Assessment (GEA) - Toward a Sustainable Future*, 1307–1400. Cambridge University Press.

Hashem, Akbari, Ryan Bell, Tony Brazel, David Cole, Maury Estes, Gordon Heisler, David Hitchcock, et al. 2016. "Reducing Urban Heat Islands: Compendium of Strategies. Urban

Heat Island Basics." Reports and Assessments. US Environmental Protection Agency. https://www.epa.gov/heat-islands/heat-island-compendium.

Herbel, Ioana, Adina-Eliza Croitoru, Adina Viorica Rus, Cristina Florina Roşca, Gabriela Victoria Harpa, Antoniu-Flavius Ciupertea, and Ionuţ Rus. 2017. "The Impact of Heat Waves on Surface Urban Heat Island and Local Economy in Cluj-Napoca City, Romania." *Theoretical and Applied Climatology* 133 (3–4): 681–95.

Herbel, Ioana, Adina-Eliza Croitoru, Ionuţ Rus, Gabriela Victoria Harpa, and Antoniu-Flavius Ciupertea. 2016. "Detection of Atmospheric Urban Heat Island through Direct Measurements in Cluj-Napoca City, Romania." *Hungarian Geographical Bulletin* 65 (2): 117–28.

Hove, L.W.A. van. 2011. *Exploring the Urban Heat Island Intensity of Dutch Cities: Assessment Based on a Literature Review, Recent Meteorological Observation and Datasets Provide by Hobby Meteorologists*. Wageningen: Alterra.

Imbroane, Alexandru. 2014. "Urban Heat Island Detection by Integrating Satellite Image Data and GIS Techniques. Case Study: Cluj-Napoca City, Romania." In .

Imbroane, Alexandru Mircea. 2018. *Sisteme informatice geografice*. Vol. 2. Cluj-Napoca: Presa Universitară Clujeană.

Irimuș, Ioan Aurel, Danuț Petrea, Ioan Rus, and Ana-Maria Corpade. 2010. "Vulnerabilitatea Spaţiului Clujean La Procesele Geomorfologice Contemporane." *Studia Universitatis Babeş-Bolyai Cluj-Napoca*, Geographia, , no. 1.

Karlessi, T., M. Santamouris, A. Synnefa, D. Assimakopoulos, P. Didaskalopoulos, and K. Apostolakis. 2011. "Development and Testing of PCM Doped Cool Colored Coatings to Mitigate Urban Heat Island and Cool Buildings." *Building and Environment* 46 (3): 570–76.

Kleerekoper, Laura, Marjolein van Esch, and Tadeo Baldiri Salcedo. 2012. "How to Make a City Climate-Proof, Addressing the Urban Heat Island Effect." *Resources, Conservation and Recycling*, Climate Proofing Cities, 64 (July): 30–38.

Kolokotsa, D., M. Santamouris, and S. C. Zerefos. 2013. "Green and Cool Roofs' Urban Heat Island Mitigation Potential in European Climates for Office Buildings under Free Floating Conditions." *Solar Energy* 95 (September): 118–30.

Landsberg, Helmut Erich. 1981. *The Urban Climate*. International Geophysics Series, v. 28. New York: Academic Press.

"Landsat User Manual 8 V 2.0." 2016. Interior Department, U.S. Geological Survey.

"Memoriu General La Planul Urbanistic General al Municipiului Cluj-Napoca." 2012. Cluj-Napoca Mayor's Office.

United Nations, and Department of Economic and Social Affairs. 2014. *World Urbanization Prospects, the 2014 Revision: Highlights*.

Oke, T. R. 1982. "The Energetic Basis of the Urban Heat Island." *Quarterly Journal of the Royal Meteorological Society* 108 (455): 1–24.

Oke, T.R. 1988. "The Urban Energy Balance." *Progress in Physical Geography* 12 (4): 471–508.

Pérez, Gabriel, Julià Coma, Ingrid Martorell, and Luisa F. Cabeza. 2014. "Vertical Greenery Systems (VGS) for Energy Saving in Buildings: A Review." *Renewable and Sustainable Energy Reviews* 39 (November): 139–65.

Sailor, David J. 1995. "Simulated Urban Climate Response to Modifications in Surface Albedo and Vegetative Cover." *Journal of Applied Meteorology* 34 (7): 1694–1704.

Santamouris, M. 2013. "Using Cool Pavements as a Mitigation Strategy to Fight Urban Heat Island—A Review of the Actual Developments." *Renewable and Sustainable Energy Reviews* 26 (October): 224–40.

Seto, Karen C., Burak Güneralp, and Lucy R. Hutyra. 2012. "Global Forecasts of Urban Expansion to 2030 and Direct Impacts on Biodiversity and Carbon Pools." *Proceedings of the National Academy of Sciences* 109 (40): 16083–88.

Sfîcă, Lucian, Adina-Eliza Croitoru, Iulian Iordache, and Antoniu-Flavius Ciupertea. 2017. "Synoptic Conditions Generating Heat Waves and Warm Spells in Romania." *Atmosphere* 8 (12): 50.

Shahmohamadi, P., A. I. Che-Ani, A. Ramly, K. N. A. Maulud, and M. F. I. Mohd-Nor. 2010. "Reducing Urban Heat Island Effects: A Systematic Review to Achieve Energy Consumption Balance." *International Journal of Physical Sciences* 5 (6): 626–36.

Sobrino, José A., J. C. Jimenez-Munoz, and Leonardo Paolini. 2004. "Land Surface Temperature Retrieval from LANDSAT TM 5." *Remote Sensing of Environment* 90: 434–40.

Song, Xiao-Peng, Joseph O. Sexton, Chengquan Huang, Saurabh Channan, and John R. Townshend. 2016. "Characterizing the Magnitude, Timing and Duration of Urban Growth from Time Series of Landsat-Based Estimates of Impervious Cover." *Remote Sensing of Environment* 175 (March): 1–13.

Stewart, I. D., and T. R. Oke. 2012. “Local Climate Zones for Urban Temperature Studies.” *Bulletin of the American Meteorological Society* 93 (12): 1879–1900.

Susca, T., S. R. Gaffin, and G. R. Dell’Osso. 2011. “Positive Effects of Vegetation: Urban Heat Island and Green Roofs.” *Environmental Pollution*, Selected papers from the conference Urban Environmental Pollution: Overcoming Obstacles to Sustainability and Quality of Life (UEP2010), 20-23 June 2010, Boston, USA, 159 (8–9): 2119–26.

Taha, Haider, Hashem Akbari, Arthur Rosenfeld, and Joe Huang. 1988. “Residential Cooling Loads and the Urban Heat Island—the Effects of Albedo.” *Building and Environment* 23 (4): 271–

Unger, János. 2004. “Intra-Urban Relationship between Surface Geometry and Urban Heat Island: Review and New Approach.” *Climate Research* 27 (MTMT:1149805): 253–64.

Weng, Qihao, Dengsheng Lu, and Jacquelyn Schubring. 2004. “Estimation of Land Surface Temperature–Vegetation Abundance Relationship for Urban Heat Island Studies.” *Remote Sensing of Environment* 89 (4): 467–83.

Xiong, Yongzhu, Shaopeng Huang, Feng Chen, Hong Ye, Cuiping Wang, and Changbai Zhu. 2012. “The Impacts of Rapid Urbanization on the Thermal Environment: A Remote Sensing Study of Guangzhou, South China.” *Remote Sensing* 4 (12): 2033–56.

Yuan, Fei, and Marvin E. Bauer. 2007. “Comparison of Impervious Surface Area and Normalized Difference Vegetation Index as Indicators of Surface Urban Heat Island Effects in Landsat Imagery.” *Remote Sensing of Environment* 106 (3): 375–86.